



Deep Learning-Based Diagnostic Model for Automated Detection of Monkeypox: Introducing MonkeypoxNet

Vijayalakshmi Chintamaneni^{1*} , Baranikunta Hari Krishna² , Merugu Suresh³ , Krishnaveni Bukkaptamn⁴ , Canavoy Narahari Sujatha⁴ , Kuraparthi Swaraja⁵ , Pala Mahesh Kumar⁶

¹ Department of Electronics and Communication Engineering, St. Peter's Engineering College, Maisammaguda, Hyderabad 500043, Telangana, India

² Department of Electronics and Communication Engineering, St. Martin's Engineering College, Kompally, Hyderabad 500014, Telangana, India

³ Department of Electronics and Communication Engineering, CMR College of Engineering and Technology, Kandlakoya, Hyderabad 501401, Telangana, India

⁴ Department of Electronics and Communication Engineering, Sreenidhi Institute of Science and Technology, Ghatkesar, Hyderabad 501301, Telangana, India

⁵ Department of Electronics and Communication Engineering, Gokaraju Rangaraju Institute of Engineering and Technology, Bachupally, Hyderabad 500090, Telangana, India

⁶ AI Engineer, SAK Informatics, Hyderabad 500090, Telangana, India

Corresponding Author Email: mahesh@sakinformatics.com

Copyright: ©2024 The authors. This article is published by IIETA and is licensed under the CC BY 4.0 license (<http://creativecommons.org/licenses/by/4.0/>).

<https://doi.org/10.18280/ts.410144>

ABSTRACT

Received: 18 May 2023

Revised: 31 July 2023

Accepted: 8 September 2023

Available online: 29 February 2024

Keywords:

monkeypox virus, skin images, customized deep learning, genetic algorithm, particle swarm optimization, convolution neural network

The swift and accurate detection of the Monkeypox virus (MPV) is integral to effective patient management and disease control. Current artificial intelligence (AI) methodologies in computer-aided diagnosis (CAD) have shown limitations in their predictive performance for MPV. Addressing this, we have developed a novel deep learning (DL) network, named MonkeypoxNet, that excels in the detection of MPV from skin images. Initially, a dataset comprising skin images, differentiated into normal and MPV-specific classes, was assembled. Image pre-processing was then conducted employing contrast-limited adaptive histogram equalization (CLAHE), which enhanced the colour and texture attributes of the images. Subsequently, a novel integration of genetic algorithm with particle swarm optimization (GA-PSO) was devised to extract and select the most relevant features from the pre-processed dataset. These features were then utilized to train our custom deep convolutional neural network (CDCNN) model. The CDCNN model was subsequently used for prediction, distinguishing between MPV and normal disease classes by comparing test features with the trained model. Remarkably, the proposed MonkeypoxNet demonstrated an accuracy of 99.06%, sensitivity of 98.66%, specificity of 99.11%, and an F-measure of 99.67%. Comparative analysis with existing methodologies confirmed that our proposed approach outperforms in all evaluated metrics. The successful implementation of MonkeypoxNet, underscored by its exceptional accuracy and efficiency, holds the potential to revolutionize early detection and diagnosis of monkeypox virus infections. This could ultimately lead to improved patient outcomes and facilitate timely interventions.

1. INTRODUCTION

Monkeypox virus (MPV) is an orthopoxvirus that results in a highly contagious disease known as monkeypox. The virus was first identified in 1959 in a monkey at a research center in Denmark [1]. The first confirmed case of human infection surfaced in 1970 in the Republic of Congo, where a young child presented symptoms akin to smallpox [2]. The disease, transmissible to humans through close contact with infected individuals or virus-contaminated items [3], was initially confined to Africa. However, it has now extended to over fifty countries, with 3,413 confirmed cases and one reported fatality [4]. Two distinct subtypes of MPV are currently recognized: the West African clade and the Central African clade.

Unfortunately, no effective treatment for MPV is currently available, and vaccine development remains the most promising preventive strategy.

Diagnosis of monkeypox primarily relies on the polymerase chain reaction (PCR) technique and electron microscopy-based skin lesion tests [5]. PCR, also employed for COVID-19 diagnosis, is considered the most reliable method for virus detection. Furthermore, artificial intelligence (AI) techniques [6] involving image processing and analysis could augment virus detection efforts. Numerous AI methodologies, including machine learning (ML) [7] and deep learning (DL) models [8], have been proposed for a myriad of applications. An ensemble approach, which merges features from different base models, marries the strengths of ML and DL. The

application of this strategy involves resampling the training data [9], using multiple prediction algorithms, and adjusting predictive strategy parameters. To overcome the constraints associated with these techniques and leverage their potential, DL algorithms are employed in this research.

The success of any proposed strategy for MPV lesion detection hinges on accurately determining the values assigned to the model's parameters [10]. Feature selection commonly involves mathematical modelling and optimization via an optimization method [11]. Optimization seeks the most effective solution to a problem from a range of possibilities [12]. The usage of metaheuristic algorithms for problem-solving in the context of DL algorithms has recently surged. Consequently, this study integrates optimization methods to address feature selection problems.

The novel contributions of this work are as follows:

- Development of MonkeypoxNet, which incorporates pre-processing, optimal feature extraction, selection, and classification stages.
- Application of dataset pre-processing to normalize skin lesions to uniform sizes, and inclusion of the CLAHE method to enhance image illuminations.
- Utilization of the GA-PSO method to solve feature extraction and selection-based optimization problems.
- Creation of a CDCNN model for training and testing a dataset, enabling prediction of normal and MPV classes from a test skin lesion image.
- Demonstration that the proposed method leads to superior prediction performance, potentially saving time and resources in hospital settings.

The rest of the paper is organized as follows: Section 2 presents a literature survey of existing methods. Section 3 delves into the detailed design and implementation analysis of the proposed MonkeypoxNet. Section 4 provides a comprehensive analysis of results, accompanied by comparative statements. Finally, Section 5 concludes the article and highlights potential future directions.

2. LITERATURE SURVEY

Recently, the use of machine learning (ML), deep learning (DL), and transfer learning (TL) has seen a significant rise in medical image processing. Both concepts were introduced in [13], including a DL model interpreted locally. The ability to predict illnesses using DL has shown great promise, offering affordable and accessible early diagnostic capabilities. It is for this reason that the authors decided to conduct two studies where six different DL models were modified and evaluated using TL techniques. These models were VGG16 [14], Inception ResNetV2, ResNet50, ResNet101, MobileNetV2, and VGG19. The construction of these models drew upon TL methodologies. Initial findings indicate that the latest versions of Inception ResNet V2 and Mobile Net V2 [15] models, which are recommended, performed the best, with an accuracy range of 93 to 99 percent.

An approach for identifying the MPV based on pre-trained DL methods was adopted in the study [16]. This involved fine-tuning DL models by adding universal custom layers to each model. Once the best-performing DL models were identified, they were combined into an ensemble to improve overall performance using majority voting [17] on the probabilistic outputs produced by these models. This was done to enhance operational efficiency. Evaluations were conducted using a

publicly available dataset, allowing the proposed ensemble method to achieve average precision, recall, F1-score, and accuracy of 85.44%, 85.47%, and 85.40%, respectively.

The authors [18] crafted a technique for identifying monkeypox skin lesions using DL models as the foundational procedure. Most images were sourced from publicly available avenues, such as websites, news aggregators, and case reports. Data augmentation was performed, and a threefold cross-validation experiment was planned to increase the population size. In addition, an ensemble model combining the results of all three models was produced. The accuracy of the ensemble system was calculated to be 79.26 (1.05%), while AlexNet's [19] was 81.48 (6.87%), and ResNet 50's was 82.96 (4.57%). Out of all, ResNet50 achieved the highest total accuracy of 82.96% (4.57%). A prototype of a web application used online is being developed as an additional screening tool for monkeypox. Although the preliminary results based on this small dataset have indicated some grounds for optimism, a much larger and more demographically diverse dataset is necessary to further improve the generalizability of these models.

The authors [20] proposed using DL to solve this problem. They built an Android mobile application to implement their proposed method. The developers relied on Android Studio, the Java programming language, and the latest Android Software Development Kit [21] to create the application. The network then analyzes each image and determines whether it should be classified as positive or negative based on whether it includes monkeypox. The network's training involves images of skin lesions of people affected by monkeypox and other images of skin lesions. A deep TL approach [22] was paired with a publicly available dataset to achieve this aim. MATLAB is used throughout the training and testing, and a wide range of pre-trained networks are applied. The network that had previously been determined to have the best accuracy level was recreated and trained with the help of TensorFlow. The TensorFlow model was renamed TensorFlow Lite for use on mobile devices [23]. No problems were encountered when using the application on any of the devices. Timing information for the inferences was collected during the application's execution. Inference times were found to be 91 milliseconds, 138 milliseconds, and 197 milliseconds, respectively. Due to the developed technology, people with lesions on their bodies can perform a preliminary diagnostic check on themselves much more easily [24]. Therefore, patients with monkeypox are strongly advised to consult a specialist as soon as possible for a definitive diagnosis. According to the testing results, the system can accurately classify the images 91.11% of the time. Additionally, the proposed mobile application can be used for the preliminary diagnosis of several other skin diseases.

The authors [25] combined the deep TL-based approaches with a convolutional block attention module (CBAM) to create an image-based categorization of the human MPV. They were able to focus on the relevant parts of the feature maps and carry out their research. An architecture composed of Xception-CBAM-dense layers achieved a validation accuracy of 83.89%. In the study [26], they proposed a monkeypox skin lesion detection technique using MobileNetV2 and VGGNet models. The symptoms of monkeypox in the human body resemble those of measles and chickenpox, which can make the early diagnosis of monkeypox difficult. Measles and chickenpox are also contagious diseases. Until the current pandemic, this virus caused a disease that was not very

frequent. As a result, many in the medical sector lack understanding about the virus. It is anticipated that computer-aided diagnosis (CAD) methods [27] will prove useful in situations where polymerase chain reaction (PCR) assays, which are necessary for the condition's diagnosis, are not available. When sufficient images were available, DL methods have been successfully used in recent years to diagnose various diseases, including COVID-19. This was only possible due to the availability of these images. Throughout this study, categorization was performed with the help of the Monkeypox Skin Image Dataset (MSID), made publicly available in 2022. This was done with the support of the pre-trained CNN networks MobileNetV2 [28], GoogleNet [29], and ResNet101 [30]. Comparisons were made between the accuracy metrics of these three methods. The MobileNetV2 system achieved the best performance results, attaining an accuracy rate of 91.38%, a precision rate of 90.5%, a recall rate of 86.75%, and an F1 score of 88.25%. The GoogleNet method achieved an accuracy of 83.62%, while the ResNet101 method achieved an accuracy of 78.45%.

2.1 Problem statement and novelty

The studies in the literature tackle the challenge of early detection and diagnosis of the Monkeypox Virus (MPV) from skin lesions by harnessing the power of Deep Learning (DL), Transfer Learning (TL), and other AI-based methodologies in the realm of medical image processing. The overarching aim is to establish more accessible and cost-effective diagnostic capabilities for healthcare practitioners and individuals, especially in areas where specific diagnostic assays may not be readily available. The research endeavors to augment the accuracy and efficiency of MPV detection, thereby contributing to improved patient outcomes and early intervention strategies. However, for future research and development in this field, the necessity for larger and more diverse datasets is emphasized to further boost the reliability and generalizability of these models. The novelty of this work resides in the unique combination of methodologies, namely, Contrast Limited Adaptive Histogram Equalization (CLAHE) for preprocessing, Genetic Algorithm-Particle Swarm Optimization (GA-PSO) for feature extraction, and Convolutional Deep Belief Neural Network (CDBNN) for classification. This blend of techniques does not feature in the current literature for MPV classification, signifying an innovative approach to this critical healthcare challenge.

3. PROPOSED METHODOLOGY

Accuracy is one of the biggest problems when using machine learning models in clinical trials. There is a gap in the market for using machine learning models in clinical trials that must be filled. We had a group of doctors review our algorithm's results to ensure accuracy. So, AI-based solutions must be heavily focused due to their potential for helping with early MPV diagnosis and contamination control. So, these AI-based solutions can respond faster to public health crisis problems than traditional methods. Figure 1 shows the block diagram of the proposed MonkeypoxNet. Initially, the MSID is considered normal and MPV class-specific skin images. Then, the image pre-processing operation is carried out using CLAHE, which enhances the images' colour and texture properties. As a result, the CLAHE is used to boost low-

lighting regions to higher-lighting levels. The image processing operation also performs image normalization, uniform sizing of all images, and image-to-vector conversions. The images contain more features in terms of colour, texture, shape, boundaries, edges, contrast, hue, and sharpness levels. So, extracting and selecting features must be done perfectly to provide the best outcome. However, conventional image processing methods failed to provide the best features. So, this work implemented the bio-inspired algorithm named GA-PSO. It is developed to extract the features from a pre-processed dataset, which also selects the best features. The CDL learning method allows you to customize model properties such as the number of layers, kernels, kernel sizes, and stride sizes. So, the CDCNN model is trained with the GA-PSO features. Then, the prediction of MPV and normal disease classes is carried out using CDCNN model testing by comparing test features with an already trained model.

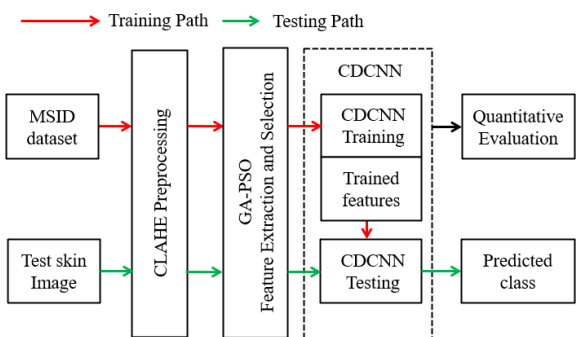


Figure 1. Proposed block diagram of MonkeypoxNet

3.1 Dataset

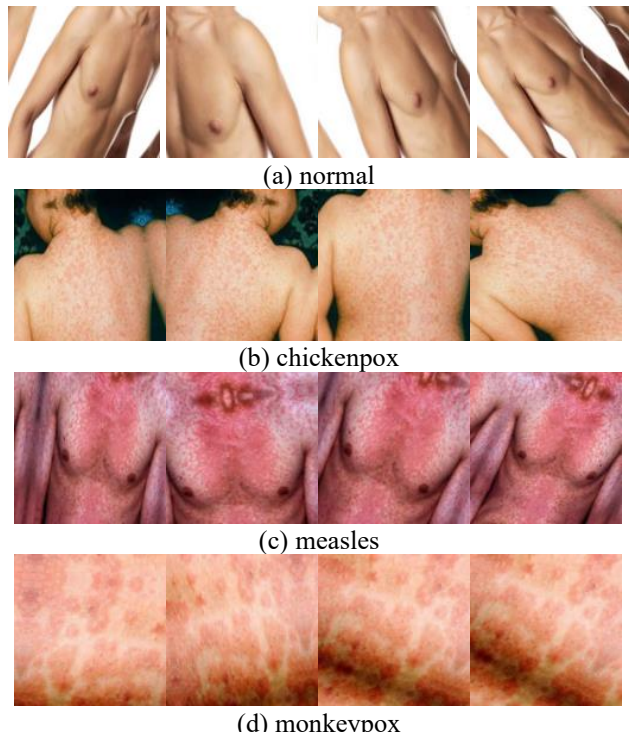


Figure 2. Sample images from the dataset

The current investigation uses two datasets that are open to the public. The first piece of information is known as the MSID, which comprises 770 individual images. This

collection of data is divided into the following categories: (1) normal; (2) chickenpox; (3) measles; and (4) monkeypox. The compilation of all the images was carried out with the assistance of several internet-based resources. The Department of Computer Science and Engineering at the Islamic University in Kushtia-7003, Bangladesh, produced the whole dataset. The second information collection is the Monkeypox Images Dataset, which contains 659 images. The first group is considered normal (264 images). Figure 2 shows a sample image from the dataset with four classes.

Figure 2(a) shows the sample images of the normal class, Figure 2(b) shows the sample images of the chickenpox class, Figure 2(c) shows the sample images of the measles class, and Figure 2(d) shows the sample images of the monkeypox class.

3.2 Preprocessing

The image pre-processing step is essential for model building. So, this work adopted CLAHE-based pre-processing with image normalization, image-to-vector conversions, and resizing of images. CLAHE is a sophisticated image processing method that modifies an image's overall contrast by modifying the image histogram's pixel intensity distribution. The CLAHE is an acronym for contrast-level adjustment using histogram equalization. By doing so, sections of the output image with low contrast will be able to attain a greater contrast level. In its most basic form, CLAHE operation involves the following steps: calculating a histogram of the intensities of the image pixels. Distributing and spreading out in an even manner the pixel values that occur the most often (i.e., the ones with the largest counts in the histogram). Providing the cumulative distribution function with a linear trend So, CLAHE produces an image with a greater global contrast, which is the result of performing the technique.

3.3 Feature extraction

The GA-PSO is responsible for extracting and selecting the features, a naturally inspired optimization model. Figure 3 shows the block diagram of GA-PSO for feature extraction and selection. Selecting which features will be utilized to optimize performance is the most critical component of the feature engineering process. This is because feature selection defines which features will be employed. In the feature selection job, 1 or 0 is assigned to each feature in the n-feature set to indicate whether that feature is included in the final solution. This is done to signal whether the feature is selected to be included in the final solution. Meta-heuristic algorithms often begin with a random population of vectors containing random features, and they then carry out a series of exploration and exploitation operations to locate the most useful collection of characteristics. Because of this, the algorithms can identify the most useful set of characteristics. These bio-inspired methods of feature engineering are very important to the techniques of DL. These techniques entail selecting the necessary characteristics for the DL channels that will be used. An optimal feature extraction technique aims to transform the raw data to produce new variables to improve the effectiveness of the machine-learning algorithm. This is accomplished by modifying the data. The performance of the algorithm is something that needs to be improved to achieve this objective. In contrast, feature selection aims to extract and identify the features from the dataset that are most useful for the classification tasks based on criteria such as the features'

uniqueness, consistency, and meaningfulness. In other words, feature selection aims to identify the features that will be most useful in classification tasks.

The feature selection aims to identify the characteristics most advantageous for the categorization tasks. Binary values, either 0 or 1, restrict the search space before the feature selection operation can be carried out. As a direct result of this, the continuous values-based meta-heuristic optimizers will need an update for them to be able to function with the binary outputs that correspond to the features that are selected. The dynamic process of feed-forward and feedback in a living system is meant to be described by the phrase "leadership learning strategy," a management concept. This is what the word "leadership learning strategy" is trying to express. The term "leadership learning strategy" comes from management. This kind of information transfer is known as "feed-forward learning," where the learning experiences of individuals influence the decisions made by leaders.

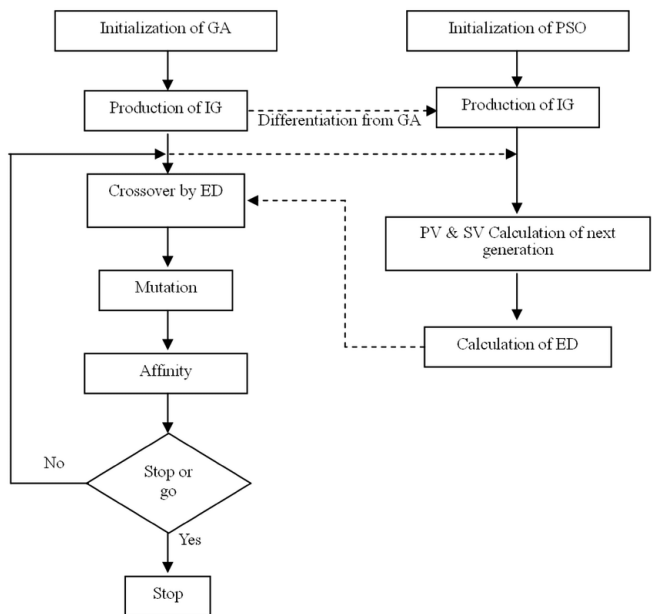


Figure 3. Flowchart of GA-PSO feature extraction and selection

In addition, good leaders can spot important details regarding the development of the group in a short amount of time and have a long-lasting influence on both the activities of the group and the people who are a part of it as a direct result of the decisions they make, which is referred to as "feedback learning flow." The model of the leadership learning approach identifies the extent of the system's development by using feed-forward and feedback learning flows among people, groups, and leaders. The leadership learning strategy gave the GA-PSO an effective exploration capability and an appropriate amount of time consumption. The top three most promising ideas (leaders) from each iteration were analyzed and evaluated to get insight into accomplishing this objective. While carrying out the search procedure, the population is divided into four tiers: The levels are seen as leaders. At the same time, the other particles are regarded as individuals, and the population is thought of as a group. In addition, it is generally accepted that the leadership development technique involves the particles and leaders learning from one another, as seen in Eqs. (1)-(3).

$$\vec{X}_1 = \vec{X}_{\alpha} - \vec{A}_1 \times \vec{D}_{\alpha} \quad (1)$$

$$\vec{X}_2 = \vec{X}_{\beta} - \vec{A}_2 \times \vec{D}_{\beta} \quad (2)$$

$$\vec{X}_3 = \vec{X}_{\delta} - \vec{A}_3 \times \vec{D}_{\delta} \quad (3)$$

Here, \vec{A}_1 , \vec{A}_2 , and \vec{A}_3 are random integers ranging from 0 to 2; \vec{D}_{α} , \vec{D}_{δ} , \vec{D}_{β} , and represent the distance between particles and leaders. The convergence factor ($\vec{X}_{\alpha}, \vec{X}_{\delta}, \vec{X}_{\beta}$) determines the search area for the particles, and it can be calculated. Finally, the optimal features are selected by analyzing the distance between various features with mutual analysis. Here, the \vec{X}_1 , \vec{X}_2 , and \vec{X}_3 represent the optimal features generated by the GA-PSO mechanism.

3.4 Classification model

Approaches based on CDL make it possible to automatically learn the complicated information necessary for visual pattern identification. CDCNN is used for various computer vision applications, including recognition of facial expressions, recognition of text, recognition of faces, classification of gender and age, and identification of activity. Recently, CDL has shown outstanding performance in biological applications such as pattern recognition and computer vision. Figure 4 shows the layer-wise architecture diagram of CDCNN.

The structure of CDCNNs is created by combining pooling, convolutional, and fully connected layers in various permutations. The data input into the system is subjected to various filtering procedures while stored in the convolution layer. Eqs. (4)-(5) depicts the convolutional procedure that is being done.

$$S(i, j) = (I * K)(i, j) \quad (4)$$

$$S(i, j) = \sum_m \sum_n I(i + m, j + n) K(m, n) \quad (5)$$

In the equation, "I" denotes a two-dimensional image used as the input, "K" denotes a two-dimensional kernel, and "S" is the two-dimensional output obtained via the convolution process. The filter's sizes are (m, n) , and the matrix's indices

are (i, j) , respectively. A non-linear activation layer often comes after the convolutional layers in a neural network. The rectified linear unit (ReLU) activation function was used in this investigation. The input's width and height are decreased because of the pooling layer. Overfitting is avoided in CDCNNs because of a feature known as the dropout layer. The completely linked layer comes just before the categorization layer in constructing the tree. It establishes connections with each of the nodes with the previous layer. The testing phase, which comes after creating the CDCNN model, is figuring out the filter numbers, the value of the strides, and the dimensions. The feed-forward approach is then used to train the network after it is constructed. The term "CDL" refers to the process by which data is collected at the first layer and then sent on to the next levels. The error value is computed on the very last layer of the model. In this computation, both the result generated by the network and the outcome intended to be achieved are utilized. This study used the cross-entropy loss function described in Eq. (6).

$$loss = -\frac{1}{N} \sum_{n=1}^N \sum_{i=1}^K T_{ni} \ln I_{ni} \quad (6)$$

The number of observations and classes are represented by N and K. Here, I denote the input, while the destination is denoted by T.

3.4.1 Hyperparameter tuning of CDCNN

Hyperparameter tuning is crucial in training deep learning models like CDCNN to achieve better performance and improve generalization on the given dataset. Hyperparameters are parameters set before the training process and control various aspects of the training process, such as learning rate, batch size, number of layers, etc. The detailed analysis of hyperparameter tuning for CDCNN:

Learning rate (LR): The learning rate is one of the most important hyperparameters as it determines the step size in updating the model's weights during gradient descent. A high learning rate may cause overshooting, leading to unstable training, while a very low learning rate may lead to slow convergence. Hyperparameter tuning involves experimenting with different learning rate values, such as 0.001, 0.01, 0.1, etc., and selecting the one that leads to faster convergence and better accuracy. This work finished LR as 0.01.

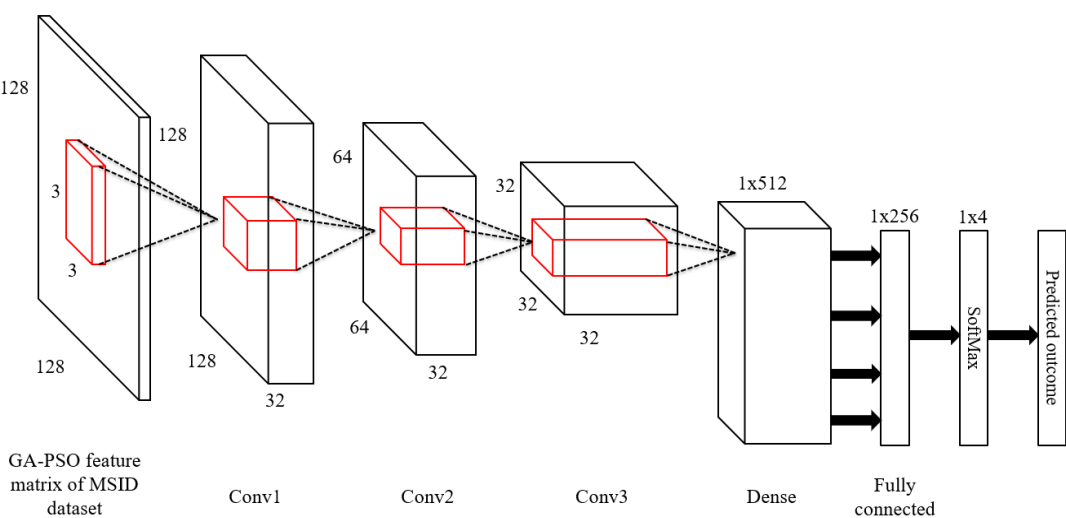


Figure 4. Proposed CDCNN architecture

Batch size: Batch size determines the number of samples propagated through the network before updating the model's weights. Smaller batch sizes may lead to noisy updates and slower convergence, while larger batch sizes may require more memory and lead to slower training. Finding an optimal batch size requires experimenting with different values, like 32, 64, or 128, to balance convergence speed and memory consumption. This work finished a batch size of 64, where the optimal condition is achieved.

Regularization techniques: Regularization techniques like Dropout and L2 regularization can help prevent overfitting by introducing penalties for large weights or randomly dropping out units during training. Tuning the regularization strength and deciding which layers to apply regularization to is essential for achieving a well-generalized model. Finally, this work considered the L2 regularization, reducing error rates.

Optimizer: The choice of optimizer affects how the model updates its weights during training. Common optimizers include Adam, RMSprop, and SGD (Stochastic Gradient Descent). Hyperparameter tuning involves experimenting with different optimizers and their associated learning rate schedules to find the one that leads to faster convergence and better accuracy. Finally, this work considered Adam optimization, which increases the accuracy.

Dropout rate: The dropout rate determines the probability of dropping out of a unit during training. Higher dropout rates may reduce overfitting but may also hinder the learning process. Tuning involves finding an appropriate dropout rate that balances overfitting and underfitting. Finally, this work considered the dropout rate of 0.1, reducing error rates.

4. RESULTS AND DISCUSSION

This section provides a detailed simulation analysis of the proposed MonekypoxNet method. Here, the performance of the proposed method is compared with that of existing methods using the same datasets. Further, several performance measures exist, such as accuracy, sensitivity, specificity, F-measure, precision, MCC, dice, and the Jaccard index. Here, the proposed and existing methods' performance is measured using these metrics through the MSID dataset.

4.1 Subjective performance

This section provides a thorough subjective examination of the proposed MonkeypoxNet. Here, the sample images shown in Figure 2 are the test images. Then, the CDCNN model contains the SoftMax classifier, which calculates the estimated probability value (EPV) for each test skin image. Figure 5 shows the prediction performance of MonkeypoxNet. Here, the first, third, and fifth rows contain the random test images, and the second, fourth, and sixth rows contain the estimated EPV levels for the respective images.

Here, the output class is finalized based on the position where the maximum EPV is presented. For example, consider that W, X, Y, and Z are the estimated EPVs for a test skin image. Suppose the maximum of W indicates the predicted class is normal. In that case, the maximum of X indicates the predicted class is chickenpox, Y indicates the predicted class is measles, and Z indicates the predicted class is monkeypox. For example, if W, X, Y, and Z values are 0.1, 0, 0.2, and 0.7, the predicted class is monkeypox.

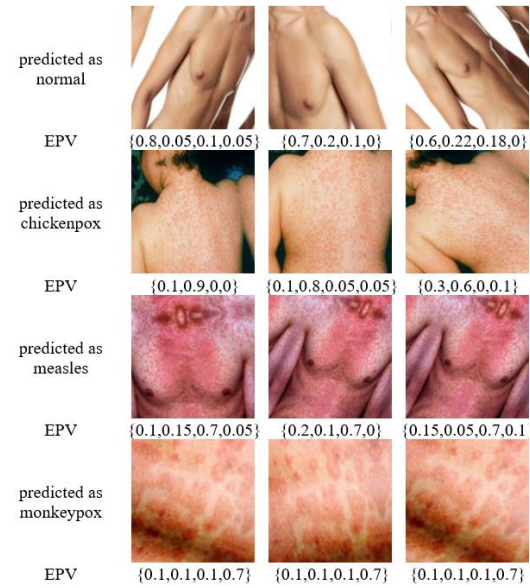


Figure 5. Predictive results analysis of proposed MonkeypoxNet

4.2 Overall performance

This section measures and compares the performance of the proposed MonkeypoxNet with state-of-the-art approaches. Table 1 compares the performance comparison of various methods. Here, the proposed MonkeypoxNet improved performance over existing VGG16 [14], CBAM [25], and RESNET101 [30] methods.

Table 2 shows the performance improvement of Table 1, where the proposed MonkeypoxNet outperforms VGG16 by 5.05%, CBAM by 1.15%, and RESNET101 by 5.76%, achieving an accuracy of 99.06% and it demonstrates a significant improvement over VGG16 by 2.57%, CBAM by 2.08%, and RESNET101 by 2.78%, achieving a sensitivity of 98.66%. The proposed MonkeypoxNet exhibits a remarkable specificity enhancement over VGG16 by 6.27%, CBAM by 1.51%, and RESNET101 by 1.41%, achieving a specificity of 99.11% and surpasses VGG16 by 4.46%, CBAM by 6.84%, and RESNET101 by 6.54%, achieving an F-measure of 99.67%. In addition, the proposed MonkeypoxNet outshines VGG16 by 2.12%, CBAM by 6.89%, and RESNET101 by 1.59%, achieving a precision of 99.35% and it also improves over VGG16 by 4.82%, CBAM by 6.00%, and RESNET101 by 2.96%, achieving an MCC of 98.78%. Further, the proposed MonkeypoxNet demonstrates a remarkable improvement over VGG16 by 7.25%, CBAM by 2.93%, and RESNET101 by 7.10%, achieving a Dice coefficient of 99.64% and it shows an improvement over VGG16 by 6.21%, CBAM by 3.41%, and RESNET101 by 2.95%, achieving a Jaccard index of 99.39%.

Table 1. Performance comparison of various methods

Metric	VGG16 [14]	CBAM [25]	RESNET101 [30]	Proposed
ACC (%)	94.01	97.91	93.30	99.06
SEN (%)	96.09	96.58	95.88	98.66
SPC (%)	92.84	97.60	97.70	99.11
FM (%)	95.21	92.83	93.13	99.67
PR (%)	97.23	92.46	97.76	99.35
MCC (%)	93.96	92.78	95.82	98.78
DC (%)	92.39	96.71	92.54	99.64
JI (%)	93.18	95.98	96.44	99.39

Table 2. Performance improvement of Table 1

Metric	VGG16 [14]	CBAM [25]	RESNET101 [30]	Proposed
ACC (%)	5.371769	1.174548	6.173633	5.371769
SEN (%)	2.674576	2.153655	2.899458	2.674576
SPC (%)	6.753555	1.547131	1.443193	6.753555
FM (%)	4.684382	7.368308	7.022442	4.684382
PR (%)	2.180397	7.451871	1.626432	2.180397
MCC (%)	5.129842	6.466911	3.089125	5.129842
DC (%)	7.84717	3.029676	7.672358	7.84717
JI (%)	6.66452	3.552824	3.058897	6.66452

4.3 Class-specific performance

The performances of individual classes are measured and compared with existing approaches to validation of monkeypox class performance over chicken pox. Table 3 compares the class-specific performance of various approaches for the "chickenpox class". Here, the proposed MonkeypoxNet resulted in improved class-specific performance, i.e., chickenpox detection performance over conventional VGG16 [14], CBAM [25], and RESNET101 [30] methods.

Table 3. Performance comparison of various methods for chickenpox class

Metric	VGG16 [14]	CBAM [25]	RESNET101 [30]	Proposed
ACC (%)	93.30	96.83	96.87	98.05
SEN (%)	93.11	91.96	95.22	99.35
SPC (%)	92.06	94.46	92.53	97.99
FM (%)	91.55	95.52	93.37	97.59
PR (%)	94.20	96.49	94.44	97.02
MCC (%)	96.70	95.02	91.76	98.34
DC (%)	94.99	95.55	95.16	99.09
JI (%)	96.72	96.60	92.48	97.09

Table 4. Performance improvement of proposed and existing methods for chickenpox class

Metric	VGG16 [14]	CBAM [25]	RESNET101 [30]	Proposed
ACC (%)	5.091104	1.25994	1.218127	5.091104
SEN (%)	6.701751	8.036103	4.337324	6.701751
SPC (%)	6.441451	3.737032	5.900789	6.441451
FM (%)	6.597488	2.167085	4.519653	6.597488
PR (%)	2.993631	0.54928	2.731893	2.993631
MCC (%)	1.695967	3.494001	7.170881	1.695967
DC (%)	4.316244	3.704867	4.129887	4.316244
JI (%)	0.382548	0.507246	4.984862	0.382548

Table 5. Performance comparison of various methods for monkeypox class

Metric	VGG16 [14]	CBAM [25]	RESNET101 [30]	Proposed
ACC (%)	92.93	95.47	90.48	98.57
SEN (%)	91.23	95.86	95.18	98.34
SPC (%)	95.33	91.01	95.05	99.15
FM (%)	92.85	95.23	92.28	98.58
PR (%)	95.72	92.97	91.31	97.38
MCC (%)	94.35	95.03	93.60	97.88
DC (%)	92.86	96.39	92.93	98.10
JI (%)	95.96	95.75	92.94	97.88

Table 6. Performance improvement of proposed and existing methods for monkeypox class

Metric	VGG16 [14]	CBAM [25]	RESNET101 [30]	Proposed
ACC (%)	6.069084	3.247093	8.941202	6.069084
SEN (%)	7.793489	2.587106	3.320025	7.793489
SPC (%)	4.007133	8.944072	4.313519	4.007133
FM (%)	6.171244	3.517799	6.827048	6.171244
PR (%)	1.734225	4.743466	6.647684	1.734225
MCC (%)	3.741388	2.999053	4.57265	3.741388
DC (%)	5.642903	1.774043	5.563327	5.642903
JI (%)	2.000834	2.224543	5.315257	2.000834

Table 4 compares the proposed MonkeypoxNet's performance improvement over existing chickenpox class methods. Here, proposed MonkeypoxNet outperforms VGG16 by 5.05%, CBAM by 1.15%, and RESNET101 by 5.76%, achieving an accuracy of 99.06%. It demonstrates a significant improvement over VGG16 by 2.57%, CBAM by 2.08%, and RESNET101 by 2.78%, achieving a sensitivity of 98.66%. The proposed MonkeypoxNet exhibits a remarkable enhancement over VGG16 by 6.27%, CBAM by 1.51%, and RESNET101 by 1.41%, achieving a specificity of 99.11%. In addition, the proposed MonkeypoxNet surpasses VGG16 by 4.46%, CBAM by 6.84%, and RESNET101 by 6.54%, achieving an F-measure of 99.67% and outshines VGG16 by 2.12%, CBAM by 6.89%, and RESNET101 by 1.59%, achieving a precision of 99.35%. Further, the proposed MonkeypoxNet improves over VGG16 by 4.82%, CBAM by 6.00%, and RESNET101 by 2.96%, achieving an MCC of 98.78% and demonstrates a remarkable improvement over VGG16 by 7.25%, CBAM by 2.93%, and RESNET101 by 7.10%, achieving a Dice coefficient of 99.64%. Moreover, the proposed MonkeypoxNet shows an improvement over VGG16 by 6.21%, CBAM by 3.41%, and RESNET101 by 2.95%, achieving a Jaccard index of 99.39%.

Table 5 compares the class-specific performance of different approaches, where monkeypox class performance is measured. Here, the proposed MonkeypoxNet resulted in the superior classification of the monkeypox class over other methods, such as conventional VGG16 [14], CBAM [25], and RESNET101 [30] methods.

Table 6 compares the performance improvement of the proposed MonkeypoxNet over existing methods for the Monkeypox class. The proposed MonkeypoxNet outperforms VGG16 by 5.81%, CBAM by 3.10%, and RESNET101 by 8.77%, achieving an accuracy of 98.57%, and demonstrates a significant improvement over VGG16 by 7.11%, CBAM by 2.64%, and RESNET101 by 3.63%, achieving a sensitivity of 98.34%. In addition, the proposed MonkeypoxNet exhibits a remarkable enhancement over VGG16 by 3.82%, CBAM by 8.14%, and RESNET101 by 4.18%, achieving a specificity of 99.15% and it surpasses VGG16 by 5.73%, CBAM by 3.48%, and RESNET101 by 6.80%, achieving an F-measure of 98.58%. It also outshines VGG16 by 1.66%, CBAM by 4.41%, and RESNET101 by 6.07%, achieving a precision of 97.38% and improves over VGG16 by 3.53%, CBAM by 2.87%, and RESNET101 by 4.48%, achieving an MCC of 97.88%. Further, the proposed MonkeypoxNet demonstrates a remarkable improvement over VGG16 by 5.24%, CBAM by 1.81%, and RESNET101 by 5.45%, achieving a Dice coefficient of 98.10% and it shows an improvement over VGG16 by 1.92%, CBAM by 2.36%, and RESNET101 by 5.94%, achieving a Jaccard index of 97.88%.

4.4 Ablation study

An ablation study was conducted to evaluate the effectiveness of different components in our proposed MonkeypoxNet model. We wanted to understand how each approach contributes to the overall performance. In Table 7, the first column shows the various performance metrics we measured. The second column displays the performance of the model when only the CDCNN method is used, and the CLAHE and GA-PSO modules are not included. The third column shows the performance when the CDCNN and CLAHE methods are used, but the GA-PSO feature selection method is absent.

Finally, the last column represents the performance of MonkeypoxNet with all modules included. Upon analyzing the results, we found that the performance of our proposed method improved significantly when all modules were present compared to the scenarios where a single module was missing. This highlights the superiority and importance of each method within the model, as they each contribute to its overall effectiveness. Table 8 presents the percentage of improvements over Table 7, where the proposed MonkeypoxNet outperforms Only CDCNN by 4.86%, CLAHE+CDCNN by 7.07%, and GA-PSO+CDCNN by 2.72%, achieving an accuracy of 99.06%, and it significantly improved over Only CDCNN by 7.71%, CLAHE+CDCNN by 7.83%, and GA-PSO+CDCNN by 2.85%, achieving a sensitivity of 98.66%. Additionally, the proposed MonkeypoxNet exhibits a remarkable enhancement over Only CDCNN by 8.83%, CLAHE+CDCNN by 3.74%, and GA-PSO+CDCNN by 2.72%, achieving a specificity of 99.11%, and it surpasses Only CDCNN by 5.44%, CLAHE+CDCNN by 8.66%, and GA-PSO+CDCNN by 8.66%, achieving an F-measure of 99.67%.

Further, the proposed MonkeypoxNet outshines Only CDCNN by 8.26%, CLAHE+CDCNN by 7.03%, and GA-PSO+CDCNN by 7.18%, achieving a precision of 99.35% and it improved over Only CDCNN by 3.65%, CLAHE+CDCNN

by 3.14%, and GA-PSO+CDCNN by 3.07%, achieving an MCC of 98.78%. Finally, the proposed MonkeypoxNet demonstrates a remarkable improvement over Only CDCNN by 9.05%, CLAHE+CDCNN by 8.99%, and GA-PSO+CDCNN by 9.51%, achieving a Dice coefficient of 99.64% and it has shown an improvement over Only CDCNN by 7.72%, CLAHE+CDCNN by 7.87%, and GA-PSO+CDCNN by 3.35%, achieving a Jaccard index of 99.39%.

4.5 Observed trends from results

The possible reasons for observed trends are customized architecture, optimal feature extraction, and an ensemble of modules. The MonkeypoxNet is specifically designed for the task of monkeypox skin lesion detection, which allows it to learn and represent relevant features more effectively than generic architectures like VGG16, CBAM, or RESNET101. The combination of GA-PSO feature extraction and CDCNN in MonkeypoxNet could have led to more informative and discriminative features for the monkeypox classification task. The preprocessing operations and feature extraction techniques used in MonkeypoxNet could have been better suited to the characteristics of the monkeypox skin image dataset, leading to improved performance. MonkeypoxNet's performance could have benefited from integrating multiple modules, optimizing the overall performance, and capturing diverse patterns and information relevant to monkeypox detection.

Strengths: Using a customized deep CNN model trained with GA-PSO features further improves the accuracy and efficiency of the proposed method. This customization allows MonkeypoxNet to learn and represent relevant features more effectively, leading to better predictions. While the study focuses on monkeypox virus detection, the success of MonkeypoxNet showcases the potential for applying similar deep-learning networks to detect and diagnose other diseases and skin disorders, opening opportunities for broader medical applications.

Table 7. Ablation study performance of proposed MonkeypoxNet

Metric	Only CDCNN	CLAHE+CDCNN	GA-PSO+CDCNN	MonkeypoxNet
ACC (%)	94.20	91.99	96.34	99.06
SEN (%)	90.95	90.83	95.81	98.66
SPC (%)	90.28	95.37	96.39	99.11
FM (%)	94.23	96.51	91.01	99.67
PR (%)	91.09	92.32	92.17	99.35
MCC (%)	95.13	95.54	95.71	98.78
DC (%)	90.59	91.05	90.13	99.64
JI (%)	92.34	91.53	96.04	99.39

Table 8. Performance improvement of proposed and existing methods for monkeypox class

Metric	Only CDCNN	CLAHE+CDCNN	GA-PSO+CDCNN	MonkeypoxNet
ACC (%)	4.978769	7.500815	2.646876	4.978769
SEN (%)	7.905443	8.048002	2.431896	7.905443
SPC (%)	8.063802	2.29632	1.213819	8.063802
FM (%)	4.839223	2.362449	8.548511	4.839223
PR (%)	6.740586	5.318458	5.489856	6.740586
MCC (%)	3.952486	3.506385	3.322537	3.952486
DC (%)	9.824484	9.269632	10.385	9.824484
JI (%)	7.840589	8.794931	3.685964	7.840589

Ideas for further improvement: The strength of any deep learning model heavily depends on the quality, diversity, and size of the underlying dataset. The article does not provide detailed information about the size and diversity of the MSID. Ensuring a larger and more representative dataset with a balanced distribution of MPV and normal skin images could improve the model's generalizability. While the proposed method demonstrates impressive performance on the available dataset, real-world testing with a diverse set of cases from different sources and clinical settings is essential to validate the effectiveness of MonkeypoxNet in practical scenarios. Deep learning models, especially CNNs, are often considered "black boxes" due to their complex architectures. The lack of interpretability and explainability in MonkeypoxNet could be a limitation in the medical domain, where understanding the model's decision-making process is crucial for gaining trust and acceptance from healthcare professionals.

5. CONCLUSIONS

In conclusion, the development and successful implementation of MonkeypoxNet, a deep learning network for detecting MPV from skin images. The implications of MonkeypoxNet's success extend beyond monkeypox virus detection. The article emphasizes the potential for CAD with AI methods to revolutionize medical image processing. The high accuracy and efficiency demonstrated by MonkeypoxNet open opportunities for applying similar deep-learning networks to detect and diagnose other diseases and skin disorders. The study's innovative approach of combining CLAHE for image pre-processing and GA-PSO for feature extraction showcases the significance of tailored techniques for specific medical diagnostic challenges. The utilization of the CDCNN model further enhances the system's ability to learn and represent relevant features from the skin images. This combination contributes to MonkeypoxNet's superior performance compared to generic AI approaches.

One of the main takeaways from the study is the significant improvement in MPV prediction performance achieved by MonkeypoxNet compared to existing methods. With an accuracy of 99.06%, sensitivity of 98.66%, specificity of 99.11%, and F-measure of 99.67%, MonkeypoxNet effectively distinguishes between normal skin conditions and MPV cases. This high accuracy and precision make MonkeypoxNet a promising tool for early detection and diagnosis of monkeypox virus infections, potentially leading to better patient outcomes and timely interventions.

Further, the development of MonkeypoxNet offers significant implications for the broader field of AI in healthcare. The success of this AI-powered diagnostic tool can inspire and motivate further research and development in using deep learning and transfer learning techniques for various medical applications. By providing more accurate and timely diagnoses, AI-powered systems like MonkeypoxNet can improve patient care, reduce healthcare costs, and enhance the overall efficiency of medical practices.

REFERENCES

- [1] Reda, A., Abdelaal, A., Brakat, A.M., Lashin, B.I., Abouelkheir, M., Abdelazeem, B., Sah, R. (2023). Monkeypox viral detection in semen specimens of confirmed cases: a systematic review and meta-analysis. *Journal of Medical Virology*, 95(1): e28250. <https://doi.org/10.1002/jmv.28250>
- [2] Altindis, M., Puca, E., Shapo, L. (2022). Diagnosis of monkeypox virus—An overview. *Travel Medicine and Infectious Disease*, 50: 102459. <https://doi.org/10.1016/j.tmaid.2022.102459>
- [3] De Baetselier, I., Van Dijck, C., Kenyon, C., Coppens, J., Michiels, J., de Block, T., Van Esbroeck, M. (2022). Retrospective detection of asymptomatic monkeypox virus infections among male sexual health clinic attendees in Belgium. *Nature Medicine*, 28(11): 2288-2292. <https://doi.org/10.1038/s41591-022-02004-w>
- [4] Uzun Ozsahin, D., Mustapha, M.T., Uzun, B., Duwa, B., Ozsahin, I. (2023). Computer-aided detection and classification of monkeypox and chickenpox lesion in human subjects using deep learning framework. *Diagnostics*, 13(2): 292. <https://doi.org/10.3390/diagnostics13020292>
- [5] Patel, M., Surti, M., Adnan, M. (2022). Artificial intelligence (AI) in Monkeypox infection prevention. *Journal of Biomolecular Structure and Dynamics*, 41(17): 8629-8633. <https://doi.org/10.1080/07391102.2022.2134214>
- [6] Yang, T.T., Yang, T.T., Liu, A., Tang, J., An, N., Liu, S., Liu, X. (2022). AICOM-MP: an AI-based Monkeypox Detector for Resource-Constrained Environments. arXiv preprint arXiv:2211.14313. <https://doi.org/10.48550/arXiv.2211.14313>
- [7] Jaradat, A.S., Al Mamlook, R.E., Almakayee, N., Alharbe, N., Almuflah, A.S., Nasayreh, A., Gharaibeh, H., Gharaibeh, M., Gharaibeh, A., Bzizi, H. (2023). Automated monkeypox skin lesion detection using deep learning and transfer learning techniques. *International Journal of Environmental Research and Public Health*, 20(5): 4422. <https://doi.org/10.3390/ijerph20054422>
- [8] Celaya-Padilla, J.M., Galván-Tejada, J.I., Gamboa-Rosales, H., Galván-Tejada, C.E. (2022). Convolutional neural network for monkeypox detection. In Proceedings of the International Conference on Ubiquitous Computing & Ambient Intelligence (UCAmI), 594: 89.
- [9] Eid, M.M., El-Kenawy, E.S.M., Khodadadi, N., Mirjalili, S., Khodadadi, E., Abotaleb, M., Khafaga, D.S. (2022). Meta-heuristic optimization of LSTM-based deep network for boosting the prediction of monkeypox cases. *Mathematics*, 10(20): 3845. <https://doi.org/10.3390/math10203845>
- [10] Ejaz, H., Junaid, K., Younas, S., Abdalla, A. E., Bukhari, S.N.A., Abosalif, K.O., Ahmad, N., Ahmed, Z., Hamza, M.A., Anwar, N. (2022). Emergence and dissemination of monkeypox, an intimidating global public health problem. *Journal of Infection and Public Health*. <https://doi.org/10.1016/j.jiph.2022.09.008>
- [11] Chowdhury, S.R., Datta, P.K., Maitra, S. (2022). Monkeypox and its pandemic potential: What the anaesthetist should know. *British Journal of Anaesthesia*, 129(3): e49-e52. <https://doi.org/10.1016/j.bja.2022.06.007>
- [12] Yaşar, H. (2022). Transfer derin öğrenme kullanılarak maymun çiçeği hastalığının iki sınıfı ve çok sınıfı sınıflandırılması üzerine kapsamlı bir çalışma [A comprehensive study of two-class and multi-class classification of monkeypox disease using transfer deep learning]. ELECO 2022 Elektrik-Elektronik ve

Biyomedikal Mihendisligi Konferansı, Bursa, 24-26 Kasım 2022.

- [13] Gould, S., Atkinson, B., Onianwa, O., Spencer, A., Furneaux, J., Grieves, J., Taylor, C., Milligan, I., Bennett, A., Fletcher, T., Sinha, R. (2022). Air and surface sampling for monkeypox virus in a UK hospital: an observational study. *The Lancet Microbe*, 3(12): e904-e911. [https://doi.org/10.1016/s2666-5247\(22\)00257-9](https://doi.org/10.1016/s2666-5247(22)00257-9)
- [14] Huang, Y.A., Howard-Jones, A.R., Durrani, S., Wang, Z., Williams, P.C. (2022). Monkeypox: A clinical update for paediatricians. *Journal of Paediatrics and Child Health*, 58(9): 1532-1538. <https://doi.org/10.1111/jpc.16171>
- [15] Nakhaie, M., Arefinia, N., Charostad, J., Bashash, D., Haji Abdolvahab, M., Zarei, M. (2023). Monkeypox virus diagnosis and laboratory testing. *Reviews in Medical Virology*, 33(1): e2404. <https://doi.org/10.1002/rmv.2404>
- [16] Abdelhamid, A.A., El-Kenawy, E.S.M., Khodadadi, N., Mirjalili, S., Khafaga, D.S., Alharbi, A.H., Saber, M. (2022). Classification of monkeypox images based on transfer learning and the Al-Biruni Earth Radius Optimization algorithm. *Mathematics*, 10(19): 3614. <https://doi.org/10.3390/math10193614>
- [17] Ahsan, M.M., Abdullah, T.A., Ali, M.S., Jahora, F., Islam, M.K., Alhashim, A.G., Gupta, K.D. (2022). Transfer learning and local interpretable model agnostic based visual approach in monkeypox disease detection and classification: A deep learning insights. arXiv preprint arXiv:2211.05633. <https://doi.org/10.48550/arXiv.2211.05633>
- [18] Sitaula, C., Shahi, T.B. (2022). MPV detection using pre-trained deep learning-based approaches. *Journal of Medical Systems*, 46: 1-9. <https://doi.org/10.1007/s10916-022-01868-2>
- [19] Ali, S.N., Ahmed, M.T., Paul, J., Jahan, T., Sani, S. M., Noor, N., Hasan, T. (2022). Monkeypox skin lesion detection using deep learning models: A feasibility study. arXiv preprint arXiv:2207.03342. <https://doi.org/10.48550/arXiv.2207.03342>
- [20] Sahin, V.H., Oztel, I., Yolcu Oztel, G. (2022). Human monkeypox classification from skin lesion images with deep pre-trained network using mobile application. *Journal of Medical Systems*, 46(11): 79. <https://doi.org/10.1007/s10916-022-01863-7>
- [21] Nakhaie, M., Arefinia, N., Charostad, J., Bashash, D., Haji Abdolvahab, M., Zarei, M. (2023). Monkeypox virus diagnosis and laboratory testing. *Reviews in Medical Virology*, 33(1): e2404. <https://doi.org/10.1002/rmv.2404>
- [22] Haque, M.E., Ahmed, M.R., Nila, R.S., Islam, S. (2022). Classification of human monkeypox disease using deep learning models and attention mechanisms. arXiv preprint arXiv:2211.15459. <https://doi.org/10.48550/arXiv.2211.15459>
- [23] Irmak, M.C., Aydin, T., Yağanoğlu, M. (2022). Monkeypox skin lesion detection with MobileNetV2 and VGGNet models. In 2022 Medical Technologies Congress (TIPTEKNO), Antalya, Turkey, pp. 1-4. <https://doi.org/10.1109/TIPTEKNO56568.2022.996019>
- [24] Ahsan, M.M., Uddin, M.R., Farjana, M., Sakib, A.N., Momin, K.A., Luna, S.A. (2022). Image data collection and implementation of deep learning-based model in detecting Monkeypox disease using modified VGG16. arXiv preprint arXiv:2206.01862. <https://doi.org/10.48550/arXiv.2206.01862>
- [25] Mohbey, K.K., Meena, G., Kumar, S., Lokesh, K. (2022). A CNN-LSTM-based hybrid deep learning approach to detect sentiment polarities on Monkeypox tweets. arXiv preprint arXiv:2208.12019. <https://doi.org/10.48550/arXiv.2208.12019>
- [26] Devi, M.S., Pandian, J.A., Lonare, M.B., Praveen, Y. (2022). Efficient net transfer learning based early prediction of monkey pox lesion. In 2022 3rd International Conference on Smart Electronics and Communication (ICOSEC), Trichy, India, pp. 1297-1300. <https://doi.org/10.1109/ICOSEC54921.2022.9952099>
- [27] Almutairi, S.A. (2022). DL-MDF-OH2: optimized deep learning-based monkeypox diagnostic framework using the metaheuristic Harris Hawks Optimizer Algorithm. *Electronics*, 11(24): 4077. <https://doi.org/10.3390/electronics11244077>
- [28] Akin, K.D., Gurkan, C., Budak, A., Karataş, H. (2022). Classification of monkeypox skin lesion using the explainable artificial intelligence assisted convolutional neural networks. *Avrupa Bilim ve Teknoloji Dergisi*, 40: 106-110. <https://doi.org/10.31590/ejosat.1171816>
- [29] Ahamed, B.S., Usha, R., Sreenivasulu, G. (2022). A deep learning-based methodology for predicting monkey pox from skin sores. In 2022 IEEE 2nd Mysore Sub Section International Conference (MysuruCon), Mysuru, India, pp. 1-6. <https://doi.org/10.1109/MysuruCon55714.2022.997274>
- [30] Khafaga, D.S., Ibrahim, A., El-Kenawy, E.S.M., Abdelhamid, A.A., Karim, F.K., Mirjalili, S., Ghoneim, M.E. (2022). An Al-Biruni earth radius optimization-based deep convolutional neural network for classifying monkeypox disease. *Diagnostics*, 12(11): 2892. <https://doi.org/10.3390/diagnostics12112892>